

Quantum beats from four-wave mixing in Rubidium 87

F.E. Becerra*, R.T. Willis, S.L. Rolston, and L.A. Orozco

*Joint Quantum Institute, Department of Physics, University of Maryland
and National Institute of Standards and Technology,
College Park, Maryland 20742, USA.*

**Departamento de Física, Centro de Investigación y de Estudios Avanzados,
Apartado Postal 14-740, México, D.F., 07000, México.*

Recibido el 26 de noviembre de 2010; aceptado el 19 de marzo de 2011

We describe the measurements of the cross-correlation function of photon pairs at 780 nm and 1367 nm showing quantum beats from Four-Wave Mixing (FWM) generated in Rubidium 87. The quantum beats come from the interference between two-photon decay paths through different intermediate hyperfine states in the process. We observe that it is possible to select different decay paths, and modify the biphoton spectra, by coupling different hyperfine levels of the atomic configuration in Rubidium with the pump fields and using selection rules.

Keywords: Four wave mixing; quantum beats; biphoton spectra.

Describimos las mediciones de funciones de correlación cruzadas de pares de fotones de longitud de onda de 780 nm y 1367 nm que muestran batimientos cuánticos de mezclado de cuatro ondas generado en rubidio 87. Los batimientos cuánticos provienen de la interferencia entre caminos de decaimiento de dos fotones a través de diferentes estados hiperfinos intermedios en el proceso. Observamos que es posible seleccionar diferentes trayectorias de decaimiento y modificar el espectro bifotónico mediante el acoplamiento de diferentes niveles hiperfinos de la configuración atómica en rubidio vía los campos de bombeo y reglas de selección.

Descriptores: Mezclado de cuatro ondas; batimientos cuánticos; espectro bifotónico.

PACS: 42.50.DV; 42.65.Ky; 42.50.Ex

1. Introduction

Long-distance quantum communication using atomic ensembles [1] requires the generation and transfer of entanglement among different ensembles. The scheme in Ref. 1 uses the interaction between single photons and atomic ensembles to transfer and extend entanglement over long distances. It has led to many theoretical and experimental investigations that focus on proving and understanding the light-matter-interaction interfaces [2,9] and the generation of entangled-photon sources for entanglement distribution among atomic ensembles [2,5]. The process of FWM generates correlations and entanglement due to the requirements of conservation of energy, linear momentum, and angular momentum [5,10]. The non-degenerate diamond configuration of the energy levels of rubidium, one ground state $5S_{1/2}$; two excited states $5P_{1/2}$ and $5P_{3/2}$; and one double excited state $6S_{1/2}$ allows the generation of light at telecommunication wavelengths (see Fig. 1). Reference 11 describes our investigation of the correlated photon pairs generated from a warm atomic ensemble of ^{85}Rb . The correlations of the photon pairs show quantum beats due to the energy levels involved in the FWM process. These quantum beats come from the interference of two possible decay paths for the photon pairs through two different hyperfine levels in the $5P_{3/2}$ in ^{85}Rb . In this article we study the generation of correlated photon pairs in ^{87}Rb . We observe quantum beats in the correlation function due to different hyperfine levels contributing to the FWM process, and we describe how to manipulate the spectral properties of the photon pairs.

When two pump beams produce a two-photon atomic excitation, a photon emitted from spontaneous emission can have a particular frequency and propagation direction that coincides with the phase matching direction for the FWM process. This excitation in the atomic ensemble increases the probability that the second photon is emitted in a direction given by the phase matching condition with a well-defined frequency, and a polarization that conserves the total angular momentum in the process. This four-photon process conserves energy and momentum so that no energy or momentum is transferred to any atom in the atomic ensemble after the four-photon interaction. The quantum state of the atom has to remain unchanged before and after the process. Then, after the two-photon excitation, there is a single final state for the atom for any possible intermediate steps for the two-photon decay. All these possibilities for the two-photon decay can interfere, and when these paths are different in frequency, the interference produces quantum beats in the correlations of the photon pairs.

We investigate the generation of correlated photon pairs from Spontaneous FWM (SFWM) in the diamond configuration of the atomic energy levels in ^{87}Rb and their temporal correlations that depend on the internal atomic structure.

This work complements Ref. 11. Here we observe quantum beats at different frequencies and broader spectrum that imply a bandwidth consistent with the measurements in Ref. 11 but with a different approach.

This paper is organized as follows. Section 2 introduces the experiment. Section 3 has the theoretical model of the

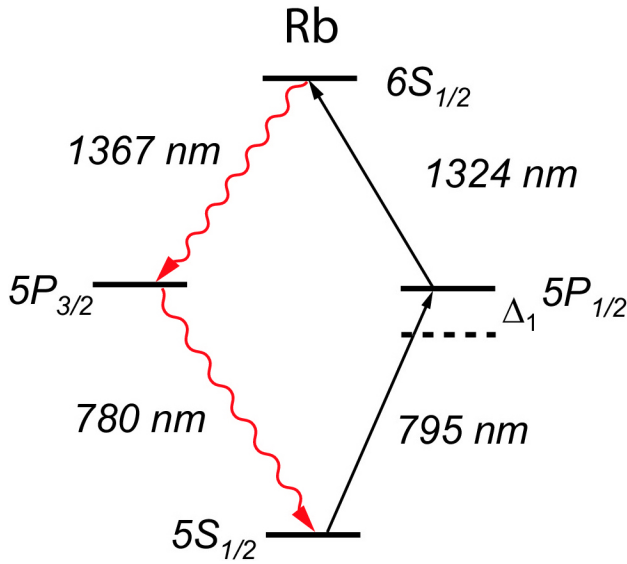


FIGURE 1. (Color online) Atomic configuration for the generation of correlated photon pairs from SFWM in Rb vapor. The pumps at 795 nm and 1324 nm produce a two-photon excitation and generate photons at 780 nm and 1367 nm from SFWM (see text for discussion).

cross correlation, Sec. 4 presents double quantum beats in the correlations and the generalized theory for them, and we conclude in Sec. 5.

2. Experiment

We generate the photon pairs from the two-photon excitation with the pump beams at 795 nm and 1324 nm and observe the two generated photons from the atomic cascade decay at 1367 nm and 780 nm propagating in the phase matching direction.

Figure 2 shows the experimental configuration for the generation of correlated photon pairs. We use a hot (100°C) isotopically pure ^{87}Rb ensemble contained in a 1.5 cm-long glass cell. We collect the correlated photon pairs from the SFWM process in the phase matching direction (see Ref. 11) into single mode fibers (SMF) at the specified wavelengths and use Avalanche Photodiodes (APD) for the detection of single photons at wavelengths of 780 nm and 1367 nm. We record the output of the APDs and analyze the correlations of the generated photon pairs.

Two beams at 795 nm and 1324 nm from two different lasers produce a two-photon excitation. The pump lasers operating in continuous wave (CW) mode are coupled to SMF and out-coupled before they overlap in the FWM rubidium cell.

We use a single photon counting module (SPCM) to detect the photons at 780 nm. This APD is a free-running non-gateable Silicon-based detector with a measured detection efficiency of $40\% \pm 10\%$. The detector for photons at 1367 nm is an In-GaAs based single photon APD running in a gated mode in order to lower the dark count rate. It is a conditional

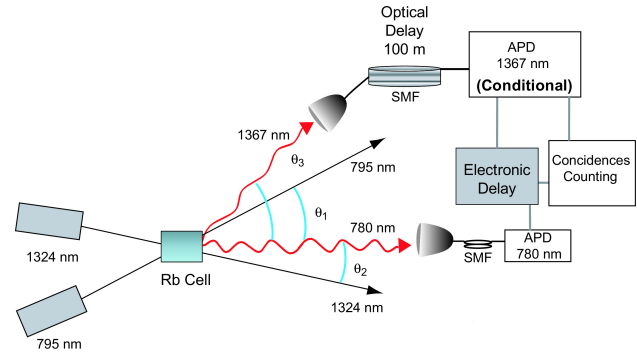


FIGURE 2. (Color online) Experimental configuration for the generation and delay coincidence studies of correlated photon pairs from SFWM in Rb vapor. The pumps at 795 nm and 1324 nm produce a two-photon excitation. APDs detect photons at 780 nm and 1367 nm in the phase matching direction with the aid of single mode fibers (SMF) to study their time correlations.

detector with a detection window of 1 ns that defines the temporal resolution of our correlation functions as 1 ns. The measured detection efficiency is $15\% \pm 5\%$.

We use coincidence counting techniques to measure the temporal correlations. We first send the photons at 1367 nm into a fiber delay line (100 m of SMF) and detect the photons at 780 nm. The transistor-transistor logic (TTL) pulse from the detector for 780 nm, after appropriate delay with a digital delay generator, triggers the detector for 1367 nm.

The optical delay is necessary for the control of the relative delay between the detection of the generated photons and the selection of the spatial mode of the generated light at 1367 nm. We use a Dual Channel Gated Photo-counter from Stanford Research (SR 400) to save the outputs of the APDs for analysis. We study the coincidences as a function of relative delay of the photon generation. We record the number of counts from photons at 780 nm and the coincidence counts as a function of relative electronic delay for a fixed collection time. The delay is set such that the overall electronic delay equals the optical delay of the photon at 1367 nm before it arrives to the APD detecting these photons (see Ref. 11 for details of the experimental implementation). We lock the frequencies of the lasers to specific atomic resonances in ^{87}Rb for particular hyperfine levels and observe the cross coincidence counts of the generated photons. We observe the counts from 780 nm photons to be about 1×10^5 counts per second, and an increase in uncorrelated coincidences in comparison to the off-resonant case described in Ref. 11.

Figure 3 shows the time-delayed coincidence counts in ^{87}Rb when the 795 nm pump laser is locked on the atomic resonance $5S_{1/2}$, $F = 2 \rightarrow 5P_{1/2}$, $F' = 1$ and the 1324 nm pump laser is locked on the atomic resonance $5P_{1/2}$, $F' = 1 \rightarrow 6S_{1/2}$, $F'' = 2$ with 200 MHz positive detuning (see Fig. 1). The time-delayed coincidence counts contain two different features: a sharp peak with a width of about 1-2 ns at zero relative delay that comes from correlated pairs of photons off resonance with the level $5P_{3/2}$; and a decaying oscillatory response at non-zero delay from pairs of photons

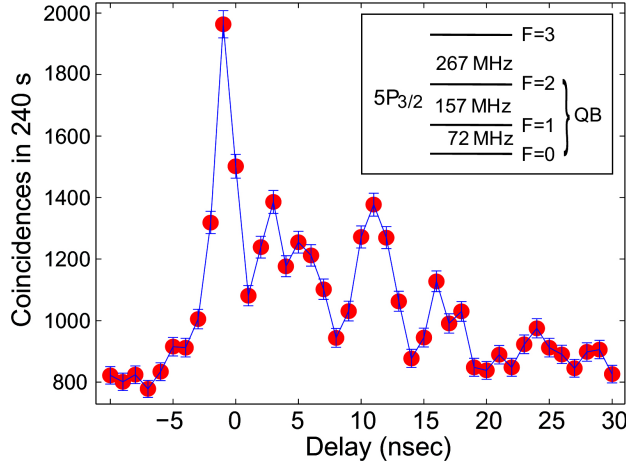


FIGURE 3. (Color online) Time-delayed coincidence counts when the pump beams couple the atomic transitions $5S_{1/2}$, $F=2 \rightarrow 5P_{1/2}$, $F'=1$ and $5P_{1/2}$, $F'=1 \rightarrow 6S_{1/2}$, $F''=2$ in ^{87}Rb . The line joins the data points, and note the suppressed zero in the vertical axis. The inset shows the hyperfine structure of the $5P_{3/2}$ atomic level indicating the quantum beat (QB).

on resonance with the level $5P_{3/2}$. Referencia 11 describes the methods used to reach this conclusion.

The generation of correlated photon pairs on resonance with the atomic level $5P_{3/2}$ results from the modification in absorption at 780 nm in the dense atomic medium caused by optical pumping. When the 795 nm pump laser is locked on the atomic transition $5S_{1/2}$, $F=2 \rightarrow 5P_{1/2}$, $F'=1$ it produces optical pumping of the atoms to the other hyperfine ground state $5S_{1/2}$, $F=1$. The absorption of the light at 780 nm changes and photons with frequencies within the Doppler width are not absorbed and reach the detector contributing to the time-delayed coincidence counts.

The modification of the absorption in the medium at 780 nm allows different two-photon decay paths from the level $6S_{1/2}$ to the level $5S_{1/2}$ resonant with different hyperfine levels of the level $5P_{3/2}$ (Inset in Fig. 3 shows the hyperfine levels of the $5P_{3/2}$ manifold). These different two-photon decay paths are in principle undistinguishable in the time-delayed coincidence counts and can produce interference. This generates quantum beats as a function of the detection delay with a beat frequency related to the energy splitting of the hyperfine levels involved in the interference process [12].

3. Theoretical model of the cross-correlation

Given the quantum state of the system $|\Psi\rangle$, the un-normalized cross correlation function (proportional to the coincidence count rate [13]) of two fields \hat{E}_1 and \hat{E}_2 is

$$|\langle 0 | \hat{E}_1^\dagger(t) \hat{E}_2^\dagger(t + \tau) | \Psi \rangle|^2 \quad [14],$$

where \hat{E}^\dagger are the positive frequency components of the field operators at the two detectors, τ is the relative delay of the photons, $|0\rangle$ is the vacuum and $|\Psi\rangle$ is the two-photon state of

the quantum field from the atomic cascade. This two-photon quantum state is calculated using the Wigner-Wesikoff approximation in a four-level atomic system consisting of a double excited state $|c\rangle$, corresponding to the hyperfine level in $6S_{1/2}$; two excited states $|b'\rangle$ and $|b''\rangle$, that correspond to the two intermediate hyperfine states of the level $5P_{3/2}$; and a ground state $|a\rangle$ corresponding to a particular hyperfine level of the atomic level $5S_{1/2}$ (See Fig. 1). We assume that the initial state of the atom is the double excited state. We solve the Schrodinger equation for this four-level atom initially in the double excited state in the presence of two vacuum fields: one corresponding to the first transition from the level $6S_{1/2}$ to the hyperfine levels in $5P_{3/2}$, and the other corresponding to the transition from these hyperfine levels to the ground state $5S_{1/2}$. We assume the long time limit and that the spectrum of the photons is centered around the resonances of the corresponding atomic transitions [14]. The probability amplitude obtained in this way when we define zero time as the time corresponding to the generation of photon 1 from the upper transition is:

$$|\langle 0 | \hat{E}_1^\dagger(t) \hat{E}_2^\dagger(t + \tau) | \Psi \rangle| = C |\exp(-i\omega_{ab'}t) + A \exp(-i\omega_{ab''}t)| \exp(-t/\tau) \quad (1)$$

where C is a normalization constant involving atomic dipole moments, atomic frequencies and densities of states of the fields [14], and we take it as a free-fit parameter since we are interested on unnormalized cross correlation functions. t is the relative delay time between the generation of photon 2, describing the photon at 780 nm resonant with the lower transition of the atomic cascade $|b\rangle \rightarrow |a\rangle$, and photon 1, describing the photon at 1367 nm resonant with the upper transition of the atomic cascade $|c\rangle \rightarrow |b\rangle$, and τ is the decay time of the correlation function. $\omega_{ab'}$ ($\omega_{ab''}$) is the optical angular frequency related to the transition energy from the ground state $|a\rangle$ to the specific hyperfine state $|b'\rangle$ ($|b''\rangle$) in the $5P_{3/2}$ and

$$A = \frac{\mu_{b''c} \mu_{ab''}^*}{\mu_{b'c} \mu_{ab'}^*}, \quad (2)$$

where μ_{ij} is the atomic dipole moment describing the relative strength of the atomic transition from the level $|i\rangle$ to the level $|j\rangle$. The parameter A can depend on the specific atomic Zeeman sublevels in the two-photon decay process, and we leave this as a free-fit parameter. In this way we account for possible differences in efficiency of the production of correlated pairs from the two different possible decay paths that will result in the reduction of the fringe visibility of the quantum beats in the correlation function [12]. We add an extra free parameter corresponding to the initial phase of the oscillations that could be due to some difference in the dispersion felt in the medium by photons with different frequencies due to the energy spacing of the two hyperfine levels of the $5P_{3/2}$ (see inset in Fig. 3).

Figure 4 shows a) the fit to the time-delayed coincidence counts, b) the normalized residuals by the standard deviation

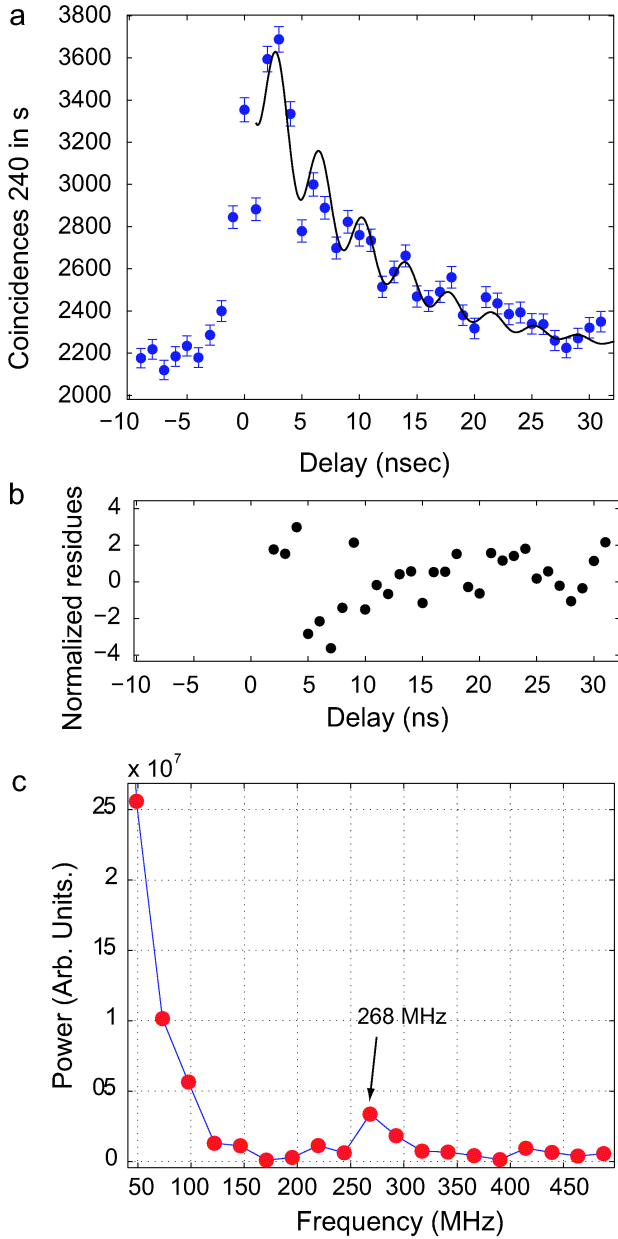


FIGURE 4. (Color online) a) Time-delayed coincidence counts with the fit to Eq. (1) as the black continuous line. b) Normalized residues. c) FFT of the coincidence counts in ^{87}Rb when the pump lasers couple the atomic transitions $5S_{1/2}$, $F = 2 \rightarrow 5P_{1/2}$, $F' = 1$ and $5P_{1/2}$, $F' = 1 \rightarrow 6S_{1/2}$, $F'' = 2$. The FFT shows a frequency component at 268 MHz corresponding to the energy splitting between the hyperfine levels $F = 2$ and $F = 3$ of the level $5P_{3/2}$.

of the count at each 1 ns bin, and c) the fast Fourier transform (FFT) of the time-delayed coincidence counts with a frequency component at 268 MHz (HWHM=25 MHz limited by the length of the time sample) that corresponds to the energy splitting of the hyperfine levels $F = 2$ and $F = 3$ of the atomic level $5P_{3/2}$ in ^{87}Rb (see inset in Fig. 3). These time-delay coincidences correspond to correlated photon pairs resonant with these specific hyperfine levels. We extract the

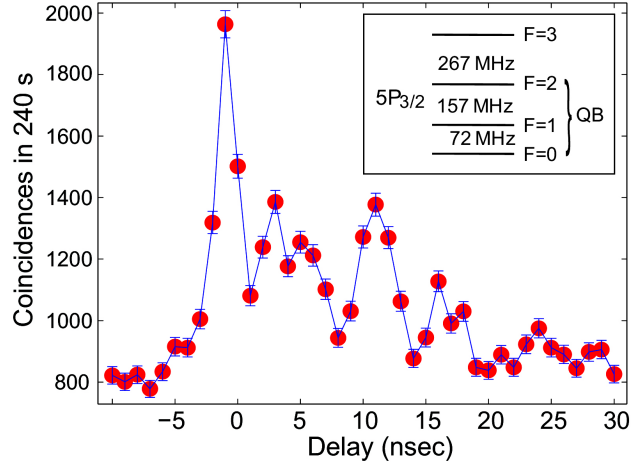


FIGURE 5. (Color online) Time-delayed coincidence counts when the pump beams couple the atomic transitions $5S_{1/2}$, $F = 1 \rightarrow 5P_{1/2}$, $F' = 2$ and $5P_{1/2}$, $F' = 2 \rightarrow 6S_{1/2}$, $F'' = 1$ in ^{87}Rb . The line joins the data points, and note the suppressed zero in the vertical axis. The inset shows the hyperfine structure of the $5P_{3/2}$ atomic level.

decay time of the coincidences using a fit to Eq. (1) with the result of $\tau = 11.07 \pm 0.2$ ns. Figure 4 a shows the fit with a reduced Chi squared $\chi^2/\text{DOF}=2.3$. We have investigated this decay time for different atomic densities ranging from $(2.4 \pm 1.2) \times 10^{11}$ to $(4.03 \pm 1.5) \times 10^{12}$ atoms per cubic centimeter, and we have not observed any change in the decay time.

Our recent work on the time response of FWM to step excitation shows decoherence and decay times faster than the atomic lifetimes involved [15] where the physical quantity of relevance is the induced atomic polarization of the sample, which is affected by Doppler broadening.

The thermal motion of the atoms, with the corresponding Doppler Shifts, shortens the decay time of the correlations [11]. Enhanced photon correlations are due to a spatial phase grating written on the collective excited atomic state in the generation process. If the atoms are moving with velocities of a few meters per second the grating begins to disappear rapidly once the atoms move a fraction of an optical wavelength shortening the correlation time of the pairs of photons.

4. Double quantum beats in ^{87}Rb

We can address different hyperfine levels of the $5P_{3/2}$ level by coupling specific hyperfine states of the levels $5S_{1/2}$, $5P_{1/2}$ and $6S_{1/2}$ with the two pump beams and by taking advantage of the angular momentum of the light (polarization) [16]. The selection of specific hyperfine states in these levels makes some hyperfine levels of $5P_{3/2}$ decouple from the FWM process and at the same time obtain new couplings to different hyperfine levels of the $5P_{3/2}$ manifold. This allows us to modify the temporal and spectral properties of the correlated photon pairs generated in ^{87}Rb .

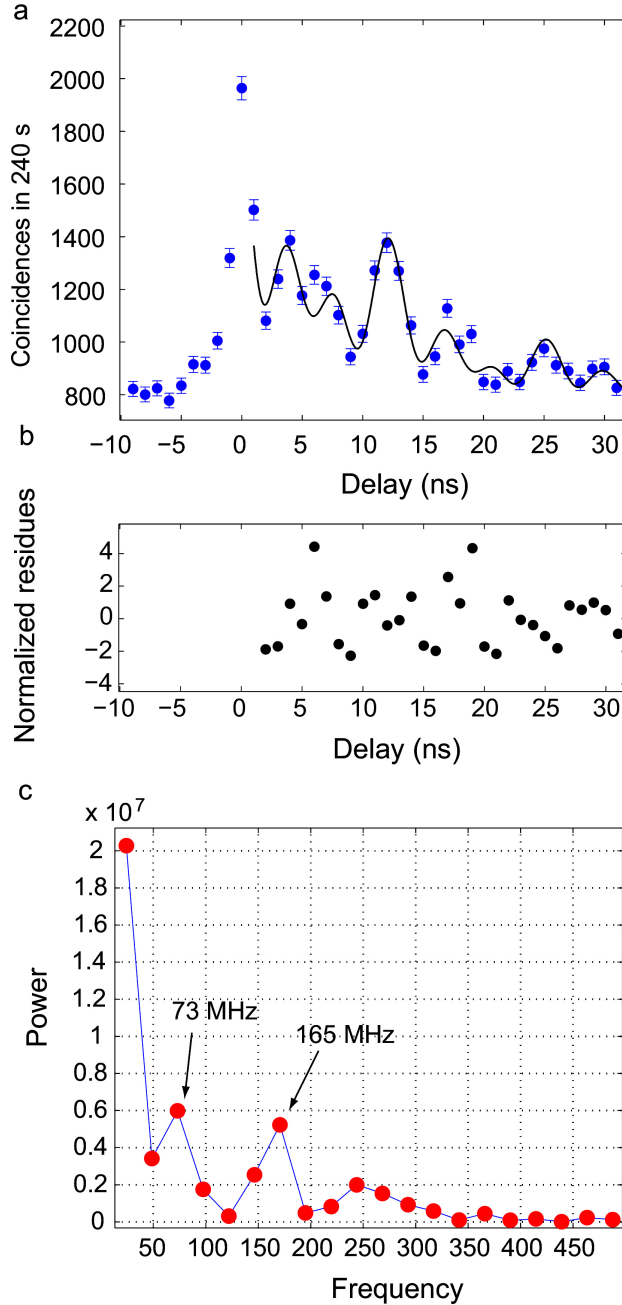


FIGURE 6. (Color online) Time-delayed coincidence counts with three intermediate hyperfine levels $F = 0$, $F = 1$ and $F = 2$ of the level $5P_{3/2}$. a) Coincidences as a function of delay with the fit in black. b) residuals. c) FFT with two peaks at 73 and 165 MHz, and also the sum of the frequencies.

Figure 5 shows the time-delayed coincidence counts of the photon pairs when we use the pump beams to couple the specific transitions: $5S_{1/2}$, $F = 1 \rightarrow 5P_{1/2}$, $F' = 2$ and $5P_{1/2}$, $F' = 2 \rightarrow 6S_{1/2}$, $F'' = 1$. This time-delayed coincidence count has two frequency components as shown in Fig. 6a: one at 73 MHz and the other at 165 MHz

(HWHM=25 MHz). These frequencies correspond to beat frequencies among three hyperfine states in the $5P_{3/2}$ atomic level; $F = 0, 1, 2$ (see inset in Fig. 5). Note that the selection of hyperfine levels in $5S_{1/2}$ and $6S_{1/2}$ decouple the hyperfine level $5P_{3/2}$, $F = 3$ from the FWM process by selection rules.

We fit the data to the function obtained from a two-photon spontaneous decay process with three possible intermediate excited states in order to estimate the correlation decay time. The calculation is analogous to the one leading to the result in Eq. (1) obtaining a probability amplitude containing three terms, with each corresponding to a specific hyperfine level. We define the time $t = 0$ at the generation of the first photon from the upper transition and we assume that the dipole strengths are the same for all the possible paths. We obtain an expression for the temporal cross-correlation function:

$$|\langle 0 | \hat{E}_1^\dagger(t) \hat{E}_2^\dagger(t + \tau) | \Psi \rangle|^2 = A_1 e^{(-t/\tau)} + A_2 [\cos(\phi_1 + \Delta_1 t/2) \times \cos(\phi_2 + \Delta_2 t/2) \cos(\phi_3 + \Delta_3 t/2)] e^{(-t/\tau)} \quad (3)$$

where ϕ_i are phases, A_i amplitudes and $\Delta_1 = \omega_{ab'} - \omega_{ab''}$, $\Delta_2 = \omega_{ab''} - \omega_{ab'''}$ and $\Delta_3 = \Delta_1 + \Delta_2$ are the splittings among all the hyperfine levels (b' , b'' , b''') = ($F=0$, $F=1$, $F=2$) in the level $5P_{3/2}$. Figure 6a shows the fit of Eq. (3) to the data with a reduced Chi squared $\chi^2/\text{DOF}=3.5$. The decay constant extracted in this way is $\tau = 14.43 \pm .38$ which is consistent with the model described in Ref. 11.

5. Concluding remarks

We have measured the structure of the time correlations on the spontaneously generated phase-matched photons from a hot atomic ensemble using rubidium 87. We observed quantum beats from the SFWM process generated from the interference of different two-photon decay paths after the two-photon excitation. The requirement of the atom to be in the same quantum state before and after the FWM process allows for the modification of the temporal and spectral properties of the photon pairs. By coupling different hyperfine levels with the pump fields and using selection rules we can select specific two-photon decay paths through different intermediate hyperfine levels. A simple model based on the Wigner-Weiskopf approximation for two-photon decay and multiple intermediate states is in good agreement with the experimental observations.

Acknowledgements

This work was supported by the NSF of the USA, DURIP of the USA, and CONACYT of Mexico.

1. L.-M. Duan, M.D. Lukin, J.I. Cirac, and P. Zoller, *Nature* **414** (2001) 413.
2. A. Kuzmich *et al.*, *Nature* **423** (2003) 731.
3. M.D. Eisaman *et al.*, *Phys. Rev. Lett.* **93** (2004) 233602.
4. M.D. Eisaman *et al.*, *Nature* **438** (2005) 837.
5. T. Chaneliere *et al.*, *Nature* **438** (2005) 833.
6. C.W. Chou *et al.*, *Nature* **438** (2005) 828.
7. T. Chaneliere *et al.*, *Phys. Rev. Lett.* **96** (2006) 093604.
8. A.G. Radnaev *et al.*, *Nature Phys.* **6** (2010) 894.
9. Y.O. Dudin *et al.*, *Phys. Rev. Lett.* **105** (2010) 260502.
10. V. Boyer, A.M. Marino, and P.D. Lett, *Phys. Rev. Lett.* **100** (2008) 143601.
11. R.T. Willis, F.E. Becerra, L.A. Orozco, and S.L. Rolston, *Phys. Rev. A* **82** (2010) 053842.
12. A. Aspect, J. Dalibard, P. Grangier, and G. Roger, *Opt. Comm.* **49** (1984) 429.
13. L. Mandel and E. Wolf, *Optical Coherence and Quantum Optics* (Cambridge University Press, New York, 1995).
14. M.S. Zubairy and M.O. Scully, *Quantum Optics* (Cambridge University Press, UK, 1997).
15. F.E. Becerra, R.T. Willis, S.L. Rolston, H.J. Carmichael, and L.A. Orozco, *Phys. Rev. A* **82** (2010) 043833.
16. D. A. Steck, Rubidium 87 D line data (<http://steck.us/alkalidata/>, as downloaded in November 13th, 2009).